DATA NORMALIZATION FOR FOUNDATION SHM OF AN OFFSHORE WIND TURBINE : A REAL-LIFE CASE STUDY

Wout Weijtjens, Tim Verbelen, Gert De Sitter, Christof Devriendt

Acoustics and Vibrations Research Group (AVRG), Vrije Universiteit Brussel, Pleinlaan 2, 1050 Brussel

wweijtje@vub.ac.be

ABSTRACT

In this contribution the first results in the development of a SHM approach for the foundations of an offshore wind turbine will be presented. Key problems are the operational and environmental variability of the resonance frequencies of the turbine. This paper suggests a (non-)linear regression model to perform data normalization. Real-life data obtained from an offshore turbine on a monopile is used to validate the used model and to demonstrate the performance of the presented approach.

KEYWORDS : *Foundation Monitoring, Offshore Wind Turbine, Operational Modal Analysis, Data normalization*

INTRODUCTION

This paper uses the results obtained from the Belwind offshore wind farm located 46km outside the Belgian coast, Fig. 1.a. The farm consists out of 55 Vestas V90-3MW turbines all on monopiles at water depths up to 30m. One of the turbines is equipped with a multiphysics sensor lay-out consisting of corrosion sensors, load and displacement sensors [2]. This contribution uses the six installed accelerometers in X-Y configuration at three different levels of the tower.

The focus of the current research lies with monitoring the foundation structure of the offshore wind turbine (OWT). The foundation is subjected to the rough offshore conditions including wave activity, the corrosive environment, currents and shifts in the sea bed. Of particular interest is the detection of scour, i.e. erosion of the seabed near the monopile.

Manual inspection of the OWT can become very expensive. As not only the OWT can be located as much as 46km offshore (e.g. Belwind), but also because the foundations are partially submerged. The combination of the harsh environment and the hard manual inspection drive the demand for a Structural Health Monitoring (SHM) solution.

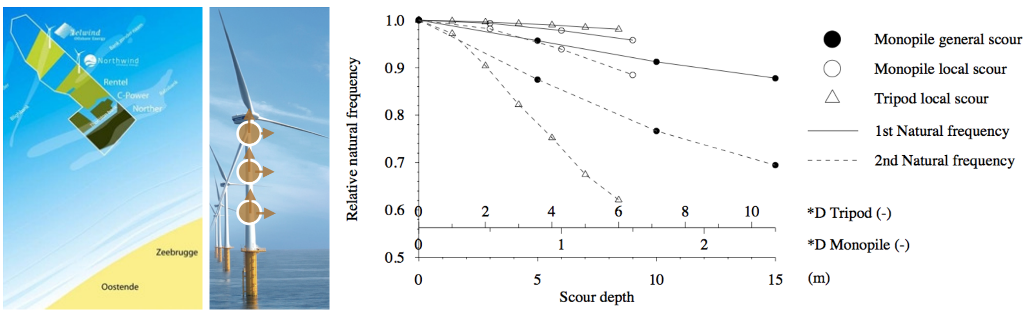

Figure 1 : Left: The Belwind windfarm is located 46km outside the Belgian coast. Center: One of the turbines at Belwind is equipped with six accelerometers in a X-Y configuration measuring vibrations in a plane parallel to the sea level. Right: Scour causes the tower resonance frequency to drop [1] for both monopile as well as tripod support structures

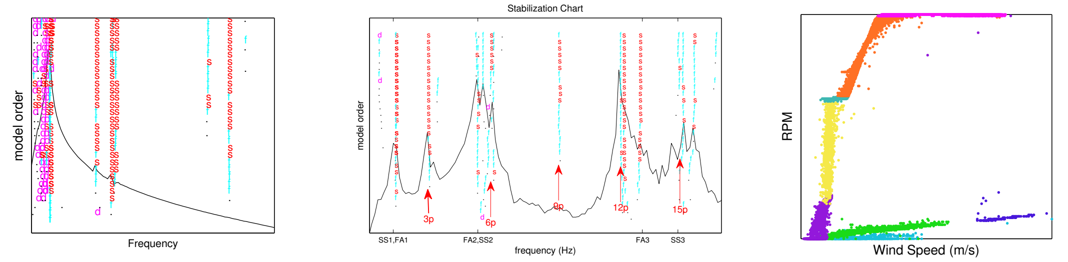

(a) Stabilization chart during parked conditions

(b) Stabilization chart at 16 rpm

(c) Example of Case definitions

Figure 2 : Rather than trying to model the strong non-linear behavior of a OWT's controller. It was opted to divide the data in different cases, different colors in (c), during which the controller is less active.

The development of such a SHM solution poses several challenges. Firstly, the foundations have often unique designs for each OWT and with variation in the soil conditions no two foundation structures will be exactly the same. Additionally it is impossible to modify or damage the structures for the sole purpose of learning patterns of damage. As such the SHM system will be designed for unsupervised learning and will, in a first step, be limited to damage recognition.
This paper will introduce the basic steps starting from the obtained resonance frequencies to a monitoring feature that is not affected by the environmental conditions.

1. METHODOLOGY

Initially data is collected and preprocessed. While statistical properties of the data are stored, frequency domain data is further used to determine the modal parameters using an automated Operational Modal Analysis (OMA), [3, 4] . For the sake of brevity, this contribution will not discuss the OMA itself. Automated OMA does allow us to have the resonance frequencies (and damping ratios) of several structural modes continuously over a long period of time. These resonance frequencies will be used as monitoring features as several studies have shown that they are directly influenced by e.g. scour, Fig. 1.c [1, 5]. However, these resonance frequencies will also vary due to environmental conditions [3] and to distinguish structural changes from the operational/environmental variability additional post-processing is required.

1.1 Reducing the effect of operational conditions

Figs.2.(a-b) show the results of an OMA measurement for a parked and rotating OWT respectively. It is clear that the dynamics of both differ significantly as the rotating blades are able to excite modes that were far less active in parked conditions. Moreover, the changed geometry (e.g. blade pitch) as well as a stronger blade-tower interaction during rotation can cause significant changes in tower resonance frequencies [4]. As a consequence it is not opportune to describe these dynamics using a single resonance frequency for the full range of operational conditions.
To reduce the operational variability it was opted to divide the data in different cases. Cases were defined by the SCADA data, Fig.2.c, with each case representing a recurring operational condition. As the geometry and operational parameters vary less within one case so do the dynamics and consequently obtaining a reduced variability within each case. More details about this case-by-case approach can be found in [4].

1.2 Reducing the effect of environmental conditions

Even within one case resonance frequencies will vary with the environmental parameters such as the wind speed, tidal-level or the wind direction. For example, the results in Fig. 3.a show a periodic variation of the resonance frequency consistent with the changing tides. While several normalization techniques exist to deal with these variabilities, an overview is available in [6], we opted to model the variability with a (non)-linear regression model.
While the first publications that used linear regression to remove environmental variability date back quite a while e.g. [7], more recent publications still apply a similar technique, e.g. [8, 9]. In previous examples the analysts installed additional wind and temperature sensors to support their monitoring campaign. This was not necessary to monitor the OWT as the turbine is equipped with several sensors for control purposes. Most relevant environmental parameters, e.g. wind speed and wind direction, are therefore known from the turbine's SCADA. The great advantage of using SCADA data is the availability of these sensors throughout the turbine's lifetime. Additional sensors are often installed within the windfarm to monitor the tidal level, wave height and temperature to assess the current meteorological conditions at the site. The same availability applies for these sensors. As such no additional environmental sensors needed to be installed.
A major advantage in the use of a (non)-linear regression model is the ease of interpretation. It is possible to assess the physicality of the applied model. For instance if a parameter is considered to be relevant to the model but has seemingly no physical meaning, then this parameter can be easily excluded from the model. This property allows both to tune the model as well as to validate it. Several examples of such validation are given in Sections 1.2.1 and 1.2.2. However, these models should never be looked at as the driving equations of the underlying physics. The models contain no physical prior-knowledge and are only the results of a data-driven (non)-linear curve fit. For example the obtained models do not take into account the interaction between environmental parameters.

1.2.1 Linear Regression

During the measurement campaign N_i environmental parameters, $Y_j(t)$, are obtained for each 10 minute interval t. These parameters can be related with the monitoring parameter, i.e. the resonance frequency of mode m , $f_m(t)$, through a linear model :

$$f_m(t) = \bar{Y}_j + \sum_{j=1}^{N_p} \alpha_j \Delta Y_j(t) \qquad \forall m \tag{1}$$

in which $Y_j(t) = \bar{Y}_j + \Delta Y_j(t)$, with $\bar{\cdot}$ the mean value. The goal of the linear regression is to find the smallest set of parameters $N_p < N_i$ that are able to adequately model the variations in f_m. The model coefficients α_j are found by solving a Total Least Squares optimization. This approach is limited to models that are linear in the coefficients (α). It however does not require models that are linear in the parameters. E.g. one could as easily use $1/Y_j$ instead of Y_j as an input to the model Eq.1.
As a proof of concept we apply a linear regression model to a set of measured resonance frequencies of the second SS mode, during a period of two weeks of parked conditions, Fig. 3.a. The linear model in Fig. 3 uses only two parameters, tidal level and wave height. Yet, it is able to model both the tidal variations within the resonance frequency as well as slower variations over time. While we should never use the obtained model as a physical representation of the system, we can use physical relations to validate the model. For example, from theory it is known that the resonance frequency will be reduced with greater tidal levels. As with higher tidal levels more of the monopile is submerged, more water gets displaced by the vibrating structure. This displaced volume acts as additional mass to the structure and will consequently reduce the resonance frequency. The true physical relation depends on the mode shapes and the mean sea level. However, this inverse relation should lead to a negative coefficient α_j associated with the tidal level. A result that is consistently obtained through different modes and datasets. And while this linear relation is not the true physical relation between resonance

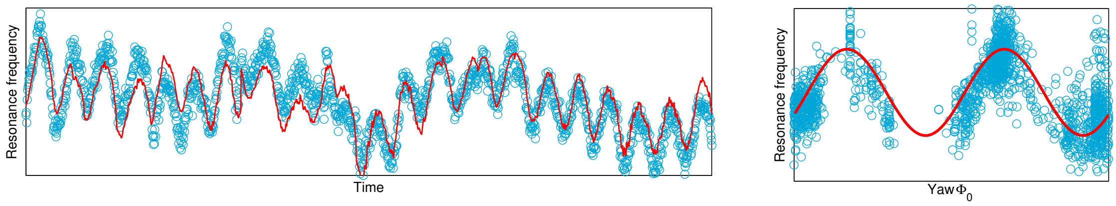

(a) Linear Model (b) Detrended

Figure 3 : (a) Even a linear model (-) can partially follow the variability in the data. (b) Looking at the normalized data reveals that the monopile is not axisymmetric

frequency and tidal level, it is sufficient to model the daily variations in the results.
In several publications the temperature, or temperature gradient, is the dominant cause of variations in the resonance frequencies [7, 8, 10]. By contrast in the current application air temperature measured at the windfarm was rarely correlated with the results. As a consequence a model expanded with air temperature never yielded any significant improvement. There are several potential explanations to this distinctive behavior. Firstly, the turbine tower is climate controlled on the inside. Secondly, the sea is a huge thermal mass of which the temperature varies very little in the course of a day. These two effects will stabilize the structures thermal balance and reduce the influence of the air-temperature upon the structure. Lastly, the structure is almost completely made out of steel, which is a good thermal conductor and only small temperature gradients will be present in the structure. Nonetheless, while the air temperature has little effect, the effect of the sea water temperature is a topic of future research and steps are being taken to acquire this data.
The final step is to subtract the obtained model from the measured data and as such partially remove the environmental variation from the measurements.

$$f_m^*(t) = f_m(t) - \sum_{j=1}^{N_p} \alpha_j \Delta Y_j(t); \tag{2}$$

From the compensated resonance frequency $f_m^*(t)$ additional physical behavior emerges. In Fig.3.b. $f_m^*(t)$ is plotted as a function of the yaw angle ϕ. A sinusoidal behavior, with a period of 180°, can be clearly seen. This implies that the structure is not fully axisymmetric, as yaw angles with higher resonance frequencies might indicate an increased stiffness in these directions. The observed variability can be modelled by incorporating the parameter $cos(2(\phi - \phi_0))$ into the model. Yet, the yaw angle with the highest resonance frequency ϕ_0 is unknown and needs to be estimated from the measurements. However, with ϕ_0 within the cosine the parameter estimation problem becomes non-linear.

1.2.2 Non-linear model

The linear regression model given in Eq.(1) is now expanded to a nonlinear model :

$$X(t) = \bar{Y}_j + \sum_{j=1}^{N_p} \alpha_j \Delta Y_j(t) + \alpha_{N_p+1} cos(2(\phi - \phi_0)) + \alpha_{N_p+2} \tag{3}$$

In which the parameters to be estimated are $\{\alpha_1, \alpha_2, \ldots, \alpha_{N_p+2}, \phi_0\}$ by means of non-linear Least squares. The initial values to this non-linear optimization can be chosen as the result of a linear estimation and a random value for ϕ_0 (e.g. 1 rad.). The additional bias coefficient α_{N_p+2} is added as $cos(2(\phi - \phi_0))$ will not be zero-mean.
Table 1 provides an overview of the models for two periods during which the turbine was parked for several days. Between both periods more than a year has passed. Each model consists out of two parameters ($N_p = 2$) , tidal level and wave height, in addition to the non-linear component as given in Eq.3.

	ϕ_0 (°)						R^2					
	FA1	SS1	FA2	SS2	FA3	SS3	FA1	SS1	FA2	SS2	FA3	SS3
Period 1	151	57	127	60.5	136	55	0,09	0,10	0,64	0,92	0,53	0,75
Period 2	161	55	126	65	147	69	0,05	0,06	0,70	0,90	0,55	0,80

Table 1 : Results of $N_p = 2$ non-linear Model for two periods of parked conditions. With R^2 the coefficient of determination and ϕ_0 the stiffest angle.

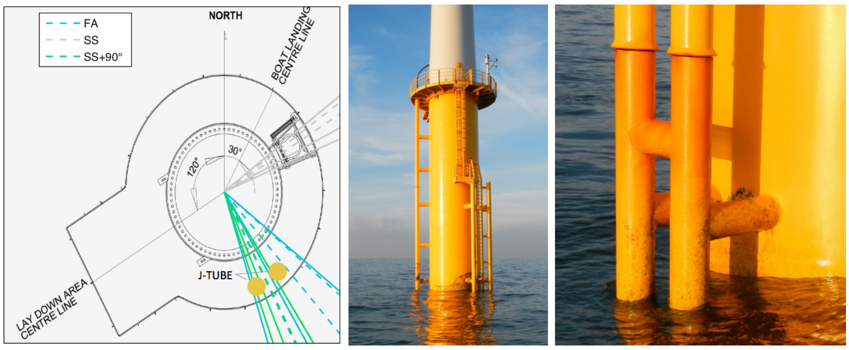

(a) Top view with indication of the stiffest angles for all 6 modes (b) Transition piece of the turbine (c) Detailed view at the J-Tube

Figure 4 : (a) All 12 values of ϕ_0 plotted on top of a top view schematic of the structures transition piece. With dashed lines for Period 1 and solid lines for Period 2. Most estimates identify the stiffest structural direction in the vicinity of the J-Tube (two yellow circles). (b) Transition piece of the turbine with on the left the J-tube and on the right the boat landing with ladders. (c) Detailed view of the J-Tube

In Table 1 it can be seen that both ϕ_0 as well as the coefficient of determination R^2 remain relatively stable between the two periods. Which indicates that the model is stable over time. A more detailed comparison between the results of Period 1 and Period 2 will be held in Section 2.
It is interesting to interpret the results for ϕ_0. ϕ_0 corresponds to the yaw angle with the highest resonance frequency. As such ϕ_0 can also be interpreted as the stiffest angle. So when the turbine is yawed at the ϕ_0 of FA1 it implies that the for-aft motion of the first mode is bending the structure in its stiffest direction. When the turbine is yawed at $\phi_0 + 180°$ the same structural components are being bent as the tower motion goes from front to back. This is consistent with the observation that both ϕ_0 as well as $\phi_0 + 180°$ have the highest resonance frequencies, Fig 3.b. For SS modes the actual side-side motion is orthogonal to the yaw angle. Implying that not ϕ_0 is the stiffest direction of the structure but $\phi_0 \pm 90°$.
Because each mode has a different mode shape, it is possible that the stiffest angles vary between modes. Nonetheless, all SS modes seem to have a stiffest angle of approximately 60°. As a consequence, the structure's stiffest direction is at 150°. This coincides with the stiffest angle of several, but not all, FA modes. In Fig.4.a a top view schematic of the considered turbine is shown. All stiffest angles are indicated by colored lines. All estimates find a structural stiffest angle close to the J-tube. Little technical detail is openly available considering the properties of the J-tube, but we do know that the J-Tube is a steel structure that runs over the entire length of the transition piece and serves to protect and guide a.o. the OWT's power cable. As such it seems plausible that this auxiliary structure stiffens the turbine.

2. Structural Health Monitoring Strategy

The structural health of the structure will be assessed by considering the structure as undamaged throughout 2012. A non-linear model as introduced in previous sections will be fitted to the resonance

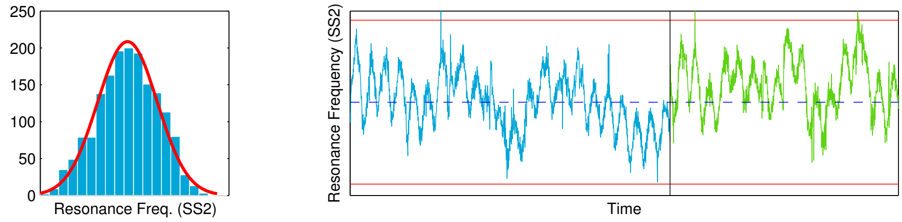

(a) Histogram of SS2 during Period 2

(b) Resonance frequency of SS2 for Period 1 (-) and Period 2 (-)

Figure 5 : A SHM approach without data-normalization does not reveal any changes within the structural properties. (left) When only looking at the histogram the data seems to be normal distributed. (right) The data of Period 2 remains within the 3σ-boundaries (horizontal red lines) of the data from Period 1

frequencies of the parked turbine, i.e. the data obtained during Period 1. This model can then be used to predict the resonance frequencies using the environmental data of the turbine during Period 2. The prediction error is used as the monitoring feature. However, first we will look at the data without applying the model.
Note that this approach can be easily applied to other operational cases and output parameters, e.g. RMS-values. However, for brevity only the resonance frequencies during parked conditions will be considered in this contribution.

2.1 SHM with unnormalized data

To demonstrate the necessity to properly address the environmental variations within the resonance frequencies, we will compare data from Period 1 with Period 2 without any normalization. In Fig.5 a normal distribution is fitted to the resonance frequencies of SS2 obtained in Period 1. While one could argue the validity of a normal distribution in the presence of significant environmental variability. The results seem to fit the distribution quite well. However, all environmental variations are present within the normal distribution, which results in a large standard deviation σ. The statistical properties of Period 1 can be used to verify the data of Period 2, Fig.5.b. While the average of Period 2 clearly exceeds that of Period 1, all data of Period 2 remains within the 3σ-boundaries. Based on these observations it could be concluded that there is little evidence of a change in the structure.

2.2 SHM with normalized data

In the previous section the available environmental data was not taken into account. Resulting in large standard deviations within the data. As discussed in Sec.1.2 it is possible to normalize the data using a low-order non-linear regression model. This model will be trained to the data of Period 1 and will then be used to predict the results of Period 2. Fig.6.b shows the results for the SS2 resonance frequencies f_{SS2}. It is clear that the prediction of the resonance frequency is significantly lower than the actual measurement.
The prediction error $e(f_{SS2,2}, \hat{f}_{SS2,2})$ between the measured results $f_{SS2,2}$ and predicted results $\hat{f}_{SS2,2}$ is used as the monitoring feature. Fig.6.a, shows that the standard deviation σ of the prediction error is far smaller than the standard deviation of the unnormalized data in gray. The prediction error of SS2 in Fig.7 clearly jumps to a larger value for Period 2. This can be caused by two things either the model is not able to properly predict the values of Period 2, or a structural change has occurred. If the bias (i.e. the mean error) between the prediction and the observations is removed, a coefficient of determination R^2 of 0.86 is found. Indicating that the model still seems to adequately predict the data. The main advantage of the current approach is that the absolute shift in the normalized frequency is rather small ($< 2\%$). Yet, due to the small σ of the prediction error this shift can still be considered

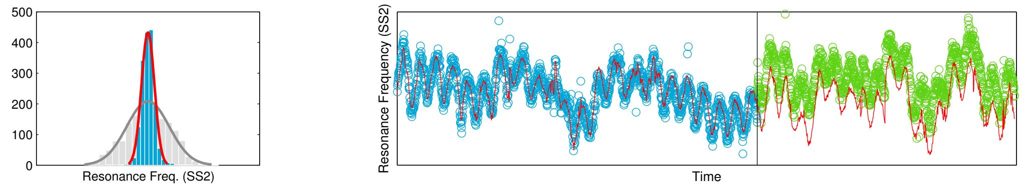

(a) Distribution of the prediction error in Period 1 (Blue), Period 2 (o)
Fig. 5.a in grayscale

(b) A model (-) trained on the data of Period 1 (o) is used to predict the values in

Figure 6 : Once data-normalization is performed using a low-order non-linear model the prediction error clearly shows a distinctive difference between both periods.

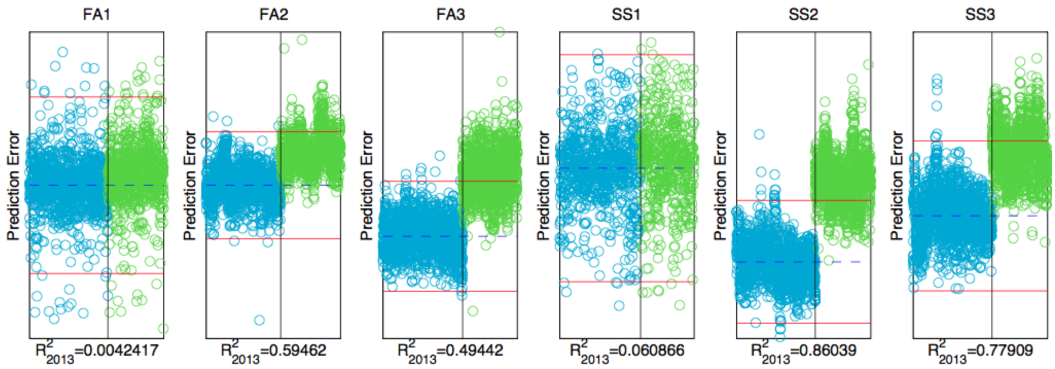

Figure 7 : Prediction Error for all 6 tower modes. In addition for each mode the R^2_{2013} value is the coefficient of determination of the prediction to the observed values with the bias between both removed.

significant as it often passes the 3σ-boundary.
While one should always address care in the physical interpretation of these results, it seems that the structure has stiffened in between the two periods. Known phenomena such as soil densification or sea bed dynamics can explain this observation. However, without further investigation they are mere hypothesis. Currently there is no real indication that the observed changes influence the turbine's performance in any way.
The results for the other modes are provided in Fig. 7. These show that for all but the lower two modes, the shifted prediction error also occur. The R^2 values do not differ significantly from the earlier R^2 values in Table 1. This indicates that the model is also able to predict the values of the other modes.

3. Future work

At this moment of time it is too soon to draw definitive conclusions about the observed variation within the data. Additional periods of stand-still have to be investigated. Especially important is whether these variations continue to progress. Or whether they can be linked to an environmental parameter that has not yet been included in the model, such as the slow varying sea water temperature. Because it is so slow varying it has little effect over the course of two weeks (length of training data), but might play a role over a longer period of time. It therefore is key to bridge the two considered periods, which differ more than a year in time. As such the introduced methodology has to be applied to all operational cases to obtain a continuous monitoring solution. Slow variations in the structural properties of the turbine can then be thoroughly investigated.
Additionally, alternative normalization algorithms will be applied in order to validate the current strategy. Simultaneously we will investigate the potential advantage of (non-linear) approaches such as Least Squares Support Vector Machines [11] or Neural Networks [12].

CONCLUSION

This contribution showed the first results of a Structural Health Monitoring approach applied to an operational off-shore wind turbine. Several physical relations validate the used model, e.g. the relation with tidal level and the identification of the turbine's stiffest angles around the J-tube. Lastly the performance of the applied normalization was compared to the results without normalization. It can be seen that there is a significant shift in most monitored resonant frequencies over the considered time span (>1 year). Future research will try to bridge the gap between the two periods and try to shed a light upon the possible cause of the observed shift.

ACKNOWLEDGEMENTS

This research has been performed in the framework of the Offshore Wind Infrastructure Project (http://www.owi-lab.be). The authors also acknowledge the financial support by the Fund for Scientific Research Flanders (FWO) and the Agency for innovation by Science and Technology (IWT). The authors gratefully thank the people of Belwind NV for their continuous support within this project.

REFERENCES

[1] MB Zaaijer and J Van der Tempel. Scour protection: a necessity or a waste of money. In *Proceedings of the 43 IEA Topixal Expert Meeting*, pages 43–51, 2004.

[2] G. De Sitter, W. Weijtjens, Y. Van Ingelgem, D. De Wilde, K. Verlinden, S. Milis, and C. Devriendt. Foundation monitoring systems: analysis of 2 years of monitoring at the north sea. Poster at EWEA 2014, March 2014.

[3] C. Devriendt, W. Weijtjens, M. El Kafafy, and G. De Sitter. Monitoring resonant frequencies and damping values of an offshore wind turbine in parked conditions. *IET Renewable Power Generation*, (In Press), 2014.

[4] W. Weijtjens, R. Shirzadeh, G. De Sitter, and C. Devriendt. Classifying resonant frequencies and damping values of an offshore wind turbine on a monopile foundation. In *Proceedings of EWEA, Barcelona*, 2014.

[5] G. Severs. Modeling and fatigue assessment of an offshore wind turbine. Master's thesis, Vrije Universiteit Brussel, 2012-2013.

[6] H. Sohn. Effects of environmental and operational variability on structural health monitoring. *Philosophical Transactions of the Royal Society A: Mathematical, Physical and Engineering Sciences*, 365(1851):539–560, 2007.

[7] B. Peeters and G. De Roeck. One year monitoring of the z24-bridge: Environmental influences versus damageevents. In *Proceedings of IMAC XVIII*, 2000.

[8] F Magalhães, A Cunha, and E Caetano. Vibration based structural health monitoring of an arch bridge: from automated oma to damage detection. *Mechanical Systems and Signal Processing*, 28:212–228, 2012.

[9] N. Martins, E. Caetano, S. Diord, F. Magalhães, and Á. Cunha. Dynamic monitoring of a stadium suspension roof: Wind and temperature influence on modal parameters and structural response. *Engineering Structures*, 59:80–94, 2014.

[10] H. Sohn, M. Dzwonczyk, E.G. Straser, A.S. Kiremidjian, K.H. Law, and T. Meng. An experimental study of temperature effect on modal parameters of the alamosa canyon bridge. *Earthquake engineering & structural dynamics*, 28(8):879–897, 1999.

[11] C.K. Oh and H. Sohn. Damage diagnosis under environmental and operational variations using unsupervised support vector machine. *Journal of Sound and Vibration*, 325(1):224–239, 2009.

[12] H. Sohn, K. Worden, and C.R. Farrar. Statistical damage classification under changing environmental and operational conditions. *Journal of Intelligent Material Systems and Structures*, 13(9):561–574, 2002.